International Journal of Electrochemical Science 20 (2025) 100923

Contents lists available at ScienceDirect

International Journal of Electrochemical Science

journal homepage: www.editorialmanager.com/ijoes

Evaluation of corrosion protection performance and color stability of environment-friendly pigmented polyurethane coating

Mamadou Ouedraogo [a,b], Tambi Ramdé [a,*], Boubié Guel [a], Stefano Rossi [b]

[a] Equipe chimie physique et électrochimie, Laboratoire de Chimie Moléculaire et de Matériaux, UFR-SEA, Université Joseph Ki-Zerbo, Ouagadougou 03 BP 7021, Burkina Faso

[b] Department of Industrial Engineering, University of Trento, Via Sommarive 9, Trento 38123, Italy

ARTICLE INFO

Keywords:
Pigment
Organic coating
Corrosion protection
Color stability
UV-ageing
Electrochemical impedance

ABSTRACT

This research is distinctive in its focus on the corrosion protection property, the ultraviolet B radiations (UV-B) resistance, and the color stability of a polyurethane (PU) base coating formulated with 1 % wt. of an environment-friendly inorganic pigment (Bi, Ca, Zn)VO_4. The pigment was synthesized and evaluated based on structure, color, and the sizes of particles. The phase composition of the synthesized pigment was studied using X-ray diffraction (XRD) analysis. Notably, the pigment's color slightly changed with its calcination's temperature, transitioning from yellow to orange. The coatings produced with a PU binder and 1 % wt. of pigment resulted in a yellow-colored coating. The color and the coating stability, as well as the barrier property of selected pigmented PU coatings, were investigated using the CIEL*a*b* color system, Fourier Transformed Infrared (FTIR) spectroscopy, and electrochemical impedance spectroscopy (EIS). The results demonstrated excellent color stability, as well as good protective barrier properties of the pigmented coating. The coatings also exhibited strong chemical stability and UV-B resistance. The high corrosion resistance and the reinforcement of the protection barrier properties of coatings were achieved via well-dispersion of the (Bi, Ca, Zn)VO_4 powder in the polymer matrix.

1. Introduction

Pigments play important roles in many fields and are mostly used to produce porcelains, ceramic tiles, printing inks, plastic, coatings, and paints [1–6]. Inorganic pigments have been widely used in various technological, architectural, and cultural domains, owing to their advantages, e.g., hiding power, weather resistance, and better thermal stability than organic dyes or pigments [7–8]. Apart from aesthetical and barrier properties associated with energy reflective capability, corrosion protection properties are also desired and sought for pigmented coatings. Pigment effectiveness could include higher tinting strength, greater ease of dispersion, better fineness of grind, higher saturation… Other properties, such as corrosion inhibition efficiency and environmental and ecological safety, are also desired. Numerous works on synthesizing and characterizing inorganic pigments have been presented in many research papers [9–15]. Parameters such as color, particle size, crystal structure, and near-infrared reflective and catalytic properties have been widely addressed in several research works. Many of these pigments can be used combined with organic coatings or paints. Beyond the specific function of a pigment, when it is associated with a paint or an organic coating applied to a metallic substrate, it will be advantageous for the pigment to have a corrosion inhibition property. Masui and co-workers have synthetized and characterized a series of environmentally friendly $Bi_{1-x-y}Ca_xZn_yVO_{4-(x+y)/2}$ $(0 \leq x \leq 0.10; 0 \leq y \leq 0.10)$ inorganic yellow pigments [1]. They found that $Bi_{0.90}Ca_{0.08}Zn_{0.02}VO_{3.95}$ had yellowness value (b*) higher than the value of a well know available bismuth vanadate ($BiVO_4$) yellow pigment and estimated that it could be an effective alternative to conventional toxic yellow pigments. It is well established that bismuth-based pigments are not dangerous to the environment and are preferable to lead, chromium, or cadmium pigment formulations. The bismuth-based pigments also offer brilliant greenish-yellow and orange shades with high opacity and color strength [16–22].

The approach to improve an organic coating performance is to enrich the polymer network with an appropriate inorganic material to obtain a highly effective and ultra-high-performance coating. Inorganic pigments are considered suitable for strengthening coating matrices to improve adhesion, hardness, strength, rigidity, and anti-corrosion activity. Polyurethanes (PUs) are widely used as coating materials in many technological domains such as biomedical, automotive, and buildings…

* Corresponding author.
E-mail address: tambi.ramde@ujkz.bf (T. Ramdé).

https://doi.org/10.1016/j.ijoes.2024.100923
Received 15 October 2024; Received in revised form 15 December 2024; Accepted 21 December 2024
Available online 25 December 2024

[23–27], due to their strong designability, film-forming ability and various physio-chemical properties. Many scientific works report on the reinforcement of PU-based coating for thermal comfort or corrosion protection purposes, but the study relating to the reinforcement of the barrier properties of PU-based coatings by the pigment (Bi, Ca, Zn)VO_4 seems not to have yet been addressed. In this work, we investigated the compatibility of (Bi, Ca, Zn)VO_4 pigment with a polyurethane (PU) base paint and the color stability of the system face to weathering. The pigment has been synthesized according to the protocol described by T. Masui and coworkers [1] and, some key parameters such as color and crystallography, which could influence some critical parameters of the coating, have been evaluated. The synthesized pigments were calcinated at different temperatures, and the resulting products were analyzed by color evaluation, X-ray diffraction (XRD), and scanning electron microscopy (SEM). The behavior of the produced coating by the UV-B aging test is also studied. Electrochemical impedance spectroscopy (EIS) has been used as an investigation tool to evaluate the corrosion protection efficiency. The structural properties of the base paint and the formulated pigmented paint are analyzed by Fourier transform infrared (FTIR) spectroscopy.

2. Experimental section

2.1. Pigment synthesis

The (Bi, Ca, Zn)VO_4 pigment was synthesized by the sol-gel route. A solution consisting of a mixture of $Bi(NO_3)_3$ 0.5 mol.L^{-1}, $Ca(NO_3)_2$ 0.1 mol.L^{-1} and $Zn(NO_3)_2$ 0.1 mol.L^{-1} were firstly prepared. 30 mL of a second solution containing HNO_3 (3 mol.L^{-1}) and 0.9 g of NH_4VO_3 were added to 25 mL of the first solution and the mixture was vigorously stirred for 30 min. The pH of the mixture was adjusted to a value of 6 by dropwise addition of aqueous ammonia (1 mol.L^{-1}) and aged for 1 h under stirring at room temperature. Then, the mixture was heated at 180 °C with a heating rate of 5 °C/min for 3 h for solvent vaporization. The resultant solid was calcined at 500, 550, 600, and 650 °C with a heating rate of 10 °C/min for 4 h. This synthesis route gives a good yield of about 65.82 ± 2.7 %. Finally, the obtained product was finely ground in an agate mortar.

2.2. Characterization

X-ray diffraction (XRD) spectra of the pigment powder were collected with a Rigaku D-Max III-D diffractometer, equipped with Cu-Kα radiation (λ = 0.154056 nm). The pigment particle morphologies were examined by SEM-EDS analysis with LEO 435VP microscope. The color coordinates of the pigment were assessed by the CIE-L*a*b* system, using a Konica Minolta CM-2600d spectrophotometer. The measurements were collected using a D65 illuminant with an observation angle of 10° and an aperture diameter of 3 mm. In the CIE-L*a*b* color scales, the L* represents the parameter of brightness or darkness of color relative to a neutral greyscale. In contrast, a* and b* parameters express qualitatively the color, respectively the red-green axis and the yellow-blue axis. Additionally, the total variation in color (ΔE*a*b*) was assessed using the equation:

$$\Delta E^* = \sqrt{(\Delta L^*)^2 + (\Delta a^*)^2 + (\Delta b^*)^2}$$

The coating thickness was collected with PHYNIX equipment, model Surfix® FN, according to the ASTM D1186–93 standard.

2.3. Coating preparation

The PU polymer used as a binder was a clear coating without pigment. This base coating was used to better evaluate the effect of the synthesized pigment on the protective properties of the coating. The solvent-borne PU coating was prepared by mixing an acrylic-based resin (Master Clear Plus CP C20 Clear), an isocyanate-based hardener (medium CCH-200), and a reducer (HiQ DR-421WS) in the ratio 2/1/0.2. The role of the hardener is to improve the adhesive force of the coating. The reducer lowers the viscosity of a coating and increases application properties.

The raw pigment was first ground to get particle sizes lower than 15 μm. The grounded pigment dispersion in the base paint was done with a high-speed propeller disperser. An optimal amount of the pigment (a ratio of 1 % wt) was added to the paint and the mixture was stirred for 10 min. The resulting paint was yellow colored. The paint was sprayed on the cold rolled steel sheets, with 70 × 70 × 1.5 mm dimensions, using a spray gun and nitrogen as a pressure gas. Before coatings, the steel panels were sandblasted, rinsed successively with acetone and demineralized water, and dried.

2.4. Color stability and protective barrier properties

The coated panels' color stability and barrier properties were evaluated during natural aging. The degradation of the formulated coating has been evaluated by FTIR spectroscopy. The measurements were performed with a Varian 4100 FTIR (Excalibur series) in reflectance mode. The resolution was 4 cm^{-1} and the spectra wavenumber ranged between 4000 – 500 cm^{-1}. The barrier property has been investigated by EIS. The EIS diagrams were recorded at the open circuit potential (OCP) using potentiostat and frequency response analyzer (FRA) equipment (AutoLab model: PG STAT 302 N). Three-electrode arrangement was used: a coated steel panel (testing area of 1 cm^2) was the working electrode, an Ag/AgCl, KCl 3 M (+ 0.197 V vs. SHE) was used as reference electrode, and the counter electrode was a platinum wire electrode. A frequency range of 10^5 – 10^{-2} Hz was explored and a 20 mV AC signal amplitude was applied. 0.5 M NaCl solution was used as an aggressive medium and, all electrochemical tests were performed at room temperature. For repeatability, three samples for each type were characterized, to ensure that, the experimental results were reproducible.

3. Results and discussion

3.1. pigment characterization

X-ray powder spectra of the (Bi, Ca, Zn)VO_4 for different calcination temperatures are shown in Fig. 1**.** The intense and sharp peaks in the diffraction spectra reveal the crystalline nature of the powder. Crystal phase qualitative analysis by QUALX 2.0 indicated a monoclinic scheelite for the pigments calcinated at 550 °C, 600 °C, and 650 °C, no diffraction peaks of impurity were observed for these spectra. For the (Bi, Ca, Zn)VO_4 calcinated at 500 °C, two crystalline structures, monoclinic and tetragonal scheelite types of $BiVO_4$, coexist.

The SEM micrographs of (Bi, Ca, Zn)VO_4 powder prepared by the sol-gel route, calcined during 4 h at temperatures ranging from 500 to 650 °C, are shown in Fig. 2**.** The microscopic aspect of the powder seems affected by the calcination temperature. With calcination of 500 °C and 550 °C, fragmentary pieces with some irregular particles can be observed (Fig. 2**a and b**). When the temperature of calcination increases, the crystallite tends to agglomerate, and larger particles with an average size of 0.5 – 0.7 μm were obtained (Fig. 2**c**). When the calcination temperature reaches 650 °C, the pigment morphology turns into a well-defined granular structure with a particle average size of 3 – 5 μm (Fig. 2**d**). EDX analyses confirm the presence of Bi, Ca, Zn, and V in the pigments.

The chromatic parameters of the (Bi, Ca, Zn)VO_4 samples obtained at various calcination temperature conditions are summarized in Table 1. All synthesized (Bi, Ca, Zn)VO_4 samples showed high yellowness values (65.8 ≤ b*≤ 88.60). The CIE-L*ab* color data for the pigments align with those obtained by previous workers [1]. The (Bi, Ca, Zn)VO_4 pigment obtained after calcination during 4 h at 500 °C and 550 °C have

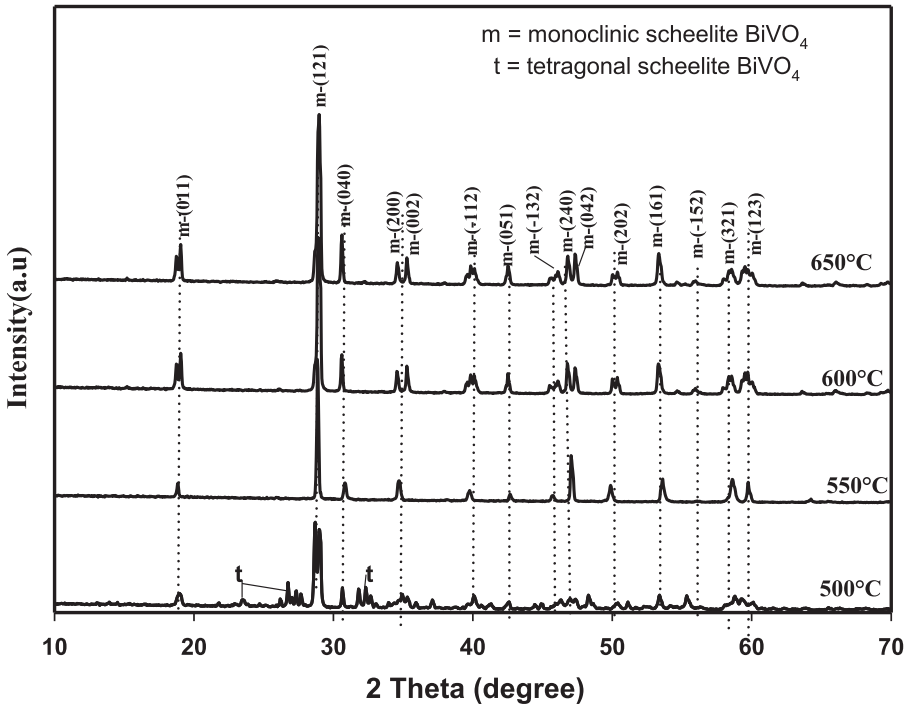

Fig. 1. Powder patterns of (Bi, Ca, Zn)VO_4 with different calcination temperatures.

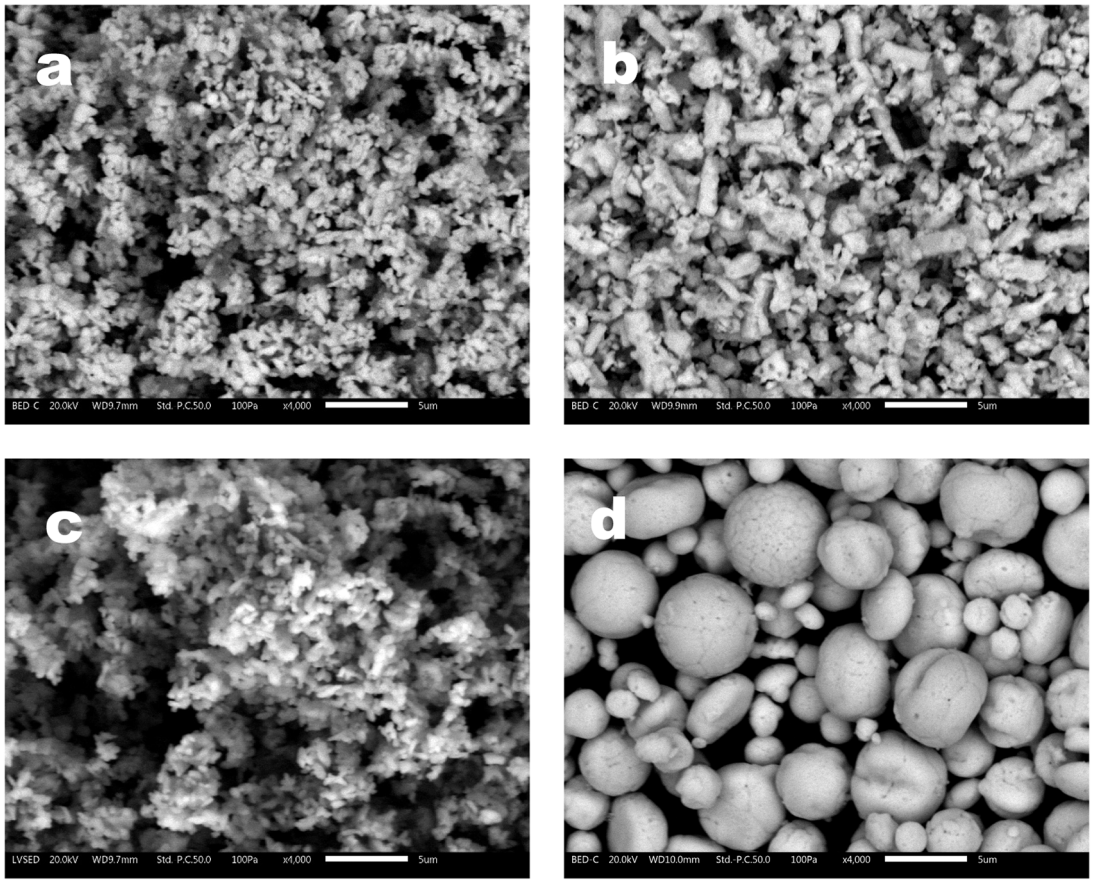

Fig. 2. SEM micrographs of $BiCaZnVO_4$ powder prepared by the sol-gel method and calcined during 4 h at 500 ∘C (**a**), 550 ∘C (**b**), 600 °C (**c**) and 650 ∘C (**d**).

Table 1
L*a*b* color coordinate of the (Bi, Ca, Zn)VO_4 samples synthesized under various conditions.

Pigments	L*	a*	b*
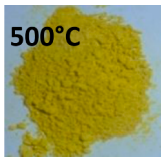	84.60 ± 0.04	5.20 ± 0.12	88.60 ± 0.05
	84.55 ± 0.04	5.15 ± 0.12	88.58 ± 0.6
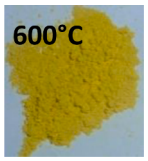	86.20 ± 0.05	3.20 ± 0.03	70.80 ± 0.04
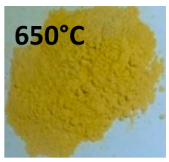	85.60 ± 0.07	2.30 ± 0.05	65.80 ± 0.09

yellowness values (respectively of 88.60 ± 0.05 and 88.58 ± 0.6) much higher than the yellowness values of a commercial $BiVO_4$ pigment (b* = 76.9). A decrease in the yellowing was observed with the increase of the calcination temperature, passing from the minimum value obtained of 88.60 (at 500 °C) to 65.80 (at 650 °C). With the naked eye, it is observed that the color changes from dark yellow to light yellow. The pigments obtained by calcination at 500 °C and 550 °C show no significant difference in color coordinates; consequently, we will further consider only the pigments obtained at 500, 600, and 650 °C.

3.2. *Coating formulation, barrier properties, and color stability evaluation*

The synthesized pigments were used for the yellow-colored coating formulations. A commercial transparent PU clear coating was used as the base paint. For each coating formulation, 1 % wt. of pigment has been used. The paint has been deposited on a steel substrate by spray coating. The thickness of the dry coating was controlled, and it was found that the thickness of all the yellow-pigmented coating was similar to the thickness of the clear PU coating, the average was about 27 μm. Incorporating the pigment in the PU polymeric binder significantly modifies all color coordinates. Table 2 presents the typical variation in color coordinates when 1 % wt. of pigment calcined at 500, 600, and 650 °C used for coating formulation. It has been observed that with the load of 1 % wt. of each type of pigment, the b* value stood high, indicating that the coating appeared very yellow.

The degree of pigment dispersion critically affects coating properties, such as surface appearance, film durability, and gloss retention [20]. The specimens used for all investigations did not present any aggregate, where the pigments were uniformly dispersed among the coating matrix without agglomerates, as presented in Fig. 3. With the same proportion of pigment −1 % wt.- the variation in color of the coating with the calcination temperature of the pigment can be clearly seen.

Table 2
L*a*b* coordinates of PU clear coating and PU + 1 % w/w calcined pigments.

	L*	a*	b*
PU clear coating	43.56	0.45	1.95
PU + 1 % wt. (Bi, Ca, Zn)VO_4 calcined at 500°C	79.51	−4.17	78.22
PU + 1 % wt. (Bi, Ca, Zn)VO_4 calcined at 600°C	75.66	−1.80	73.81
PU + 1 % wt. (Bi, Ca, Zn)VO_4 calcined at 650°C	72.06	0.97	67.72

The comparison between the FTIR spectra of the base PU clear coating and the pigmented coatings obtained with 1 % wt. of (Bi, Ca, Zn)VO_4 calcined at different temperatures is represented in Fig. 4. As it can be seen, no significant change in FTIR spectra was observed with the pigments load, except the coating made with the pigment calcined at 500 °C where the C═O vibration band at 1725.12 cm^{-1} appears as a singlet, whereas it exists in the form of a doublet in the other cases. The presence of the doublet carbonyl absorption band can be attributed to one or more of the following reasons [21–25]: (i) intermolecular associations; (ii) intramolecular effects; accidental or near-degeneracy of carbonyl fundamental with another fundamental, overtone, or combination band of different symmetry (no Fermi resonance occurs), (iii) Fermi resonance, due to accidental or near degeneracy of carbonyl fundamental with overtone or combination band of same symmetry. Due to the tiny amount of pigment used, this is well justified since those of the PU polymer drown the absorption bands from the structure of the

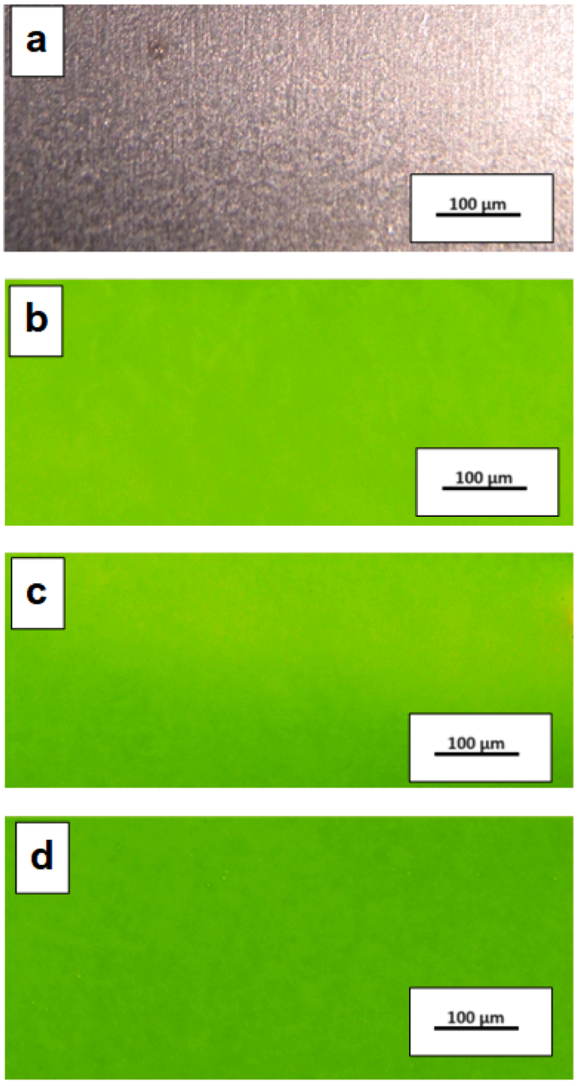

Fig. 3. appearance of coated specimens by optical microscopy; (**a**): clear-coated specimen and PU + 1 % wt. (Bi, Ca, Zn)VO_4 pigment respectively calcined at 500 °C (**b**); 600 °C (**c**) and 650 °C (**d**).

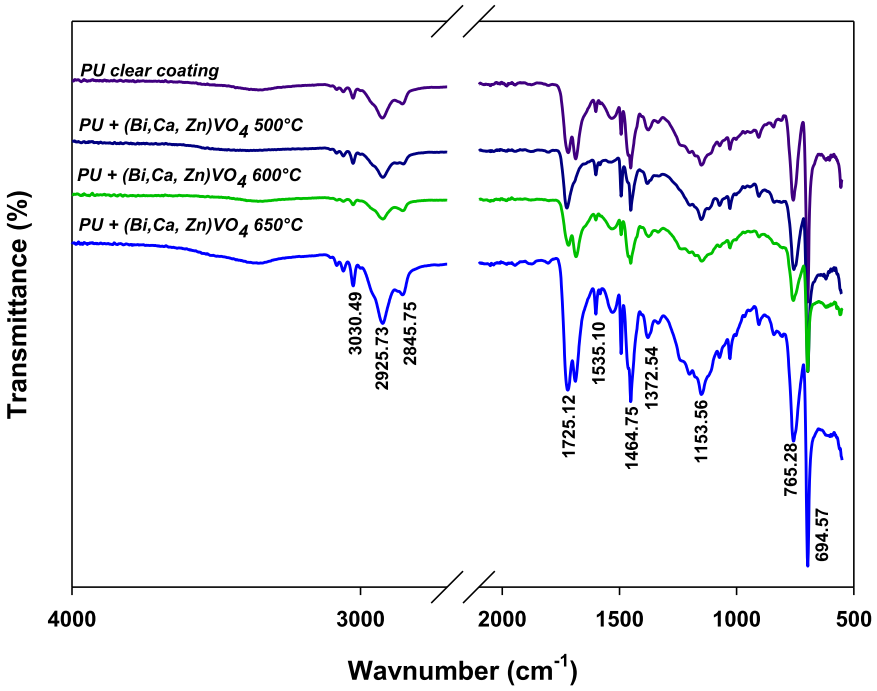

Fig. 4. FTIR spectra of PU clear coating and PU+ 1 % wt. (Ba, Ca, Zn)VO_4 calcined at different temperatures.

pigment. The peaks observed at 2957 cm^{-1} and 2742 cm^{-1} are due to the C–H aliphatic stretching of the polymer [26]. The small peak observed at 1533 cm^{-1} is assigned to the carbamate group (−NH−COO−), while the peak at 1465 cm^{-1} belongs to C-H bending. The large band at 1153 cm^{-1} correlates to C–C/C–O bond stretching [26]. The peak observed at 765 cm^{-1} is attributed to C–H rock bending [26].

EIS measurements were conducted to evaluate the corrosion protection performance of the coatings. The measurement was performed on coated steel panels immersed in a NaCl 0.5 M solution. Fig. 5 shows the Bode modulus (**a**) and Bode phase (**b**) plots for the coated steel immediately after immersion. Fig. 5**a** shows that the Bode modulus plot of the pigmented coatings exhibited a straight-line behavior with a slope of – 1 the whole frequency range, and the low-frequency magnitude of $|Z|_{0.01\ Hz}$ is about 10^{10} Ω.cm^2. This indicates that these samples have excellent barrier properties and good intactness on the metallic substrate. The Bode modulus plot exhibits an inflection at the low-frequency domain at about log (f) ~ 0.25 Hz for the clear coating system. This trend is observed on the Bode phase plot (Fig. 5**b**), where a drop in the phase angle value in the low-frequency domain was observed and associated with a second-time constant. Nevertheless, the Bode modulus graphs of the clear show a quasi-capacitive behavior for a wide range of frequencies, and its $|Z|_{0.01\ Hz}$ magnitude remains considerably high (~ 10^9 Ω.cm^2), indicating a protective barrier property.

An ideal protective coating displays a capacitive impedance which depends on the frequency. This behavior is equivalent to an R(QR) type electrical circuit (Fig. 6**a**), this model of equivalent fits the impedance data well at the very first time of immersion. For a metal-organic coating system, in prolonged immersion conditions, the suitable equivalent electrical circuit is the R(Q(R(QR))) type, represented in Fig. 6**b**. R_s is the resistance of the corrosive solution, Q_{dl} is a constant angle phase element, and R_{ct} represents the charge transfer resistance. These circuit elements characterize the metal-coating interface. The solution-coating interface is characterized by the circuit elements Q_f and R_f which represent the constant phase element and the resistance of the organic coating, respectively. Q is a constant phase element (CPE), used instead of pure capacitance to account for non-ideal behaviors of the electrode system. Deviations from ideal behavior can be classified into two groups: (i) a distortion of current and/or potential distributions at the interface or slow kinetics for the adsorption of charged species; (ii) inhomogeneities of the electrode surface such as roughness, electrode porosity and variable coating composition [27–29]. The impedance for a CPE is expressed as follows [30]:

$$Z_{CPE} = \frac{1}{Y_0}(j\omega)^{-n}$$

Y_0 and n are corrective parameters where $-1 \leq n \leq 1$. Depending on the value of n, the *CPE* can represent an inductance ($n = -1$), a resistance ($n = 0$), a Warburg impedance ($n = 1/2$), or a pure capacitor ($n = 1$). For impedance data fitting, ZsimpWin 3.50 software has been used in this study.

Fig. 7 reports the plot of the impedance modulus and the phase angle over a long immersion time in 0.5 M NaCl solution for a steel substrate coated with PU clear coating and with PU coating containing the (Bi, Ca, Zn)VO_4 pigment calcined at different temperature. For all pigmented coating, the $|Z|_{0.01\ Hz}$ value is about 1.28×10^{10} Ω.cm^2 immediately after immersion. It appears that the calcination temperature of the pigment and, therefore, the difference in size and grain shape of the pigment microparticles does not affect the protective properties of the coating. The $|Z|_{0.01\ Hz}$ value off all pigmented coating systems remains high after 720 h immersion time in the solution, indicating good stability of the painting system and a good protective barrier to aggressive species. The values of the pseudo-capacitance Y_0, obtained from impedance data fitting, were about 10^{-10} $S.sec^{-n}$ for pigmented coating systems while for clear coating, Y_0 was about 10^{-9} $S.sec^{-n}$. The decrease in the pseudo-capacitance value for pigmented coating systems reflected a less active interface, indicating better coating stability.

The phase angle presents one time constant and shows evident changes after about 720 h of immersion time test (Fig. 7**a, b, c, and d**). The high phase angle values exhibited by the pigmented coating system indicate a capacitive response of the system. After about 720 h of immersion in 0.5 M NaCl, a second-time constant appeared in the phase angle. This is attributed to charge transfer reactions at the interface between the coating and steel substrate, suggesting that the electrolyte reaches the steel substrate through defects. This indicates that (Bi, Ca, Zn)VO_4 1 % wt. pigmented coating is an efficient corrosion protective

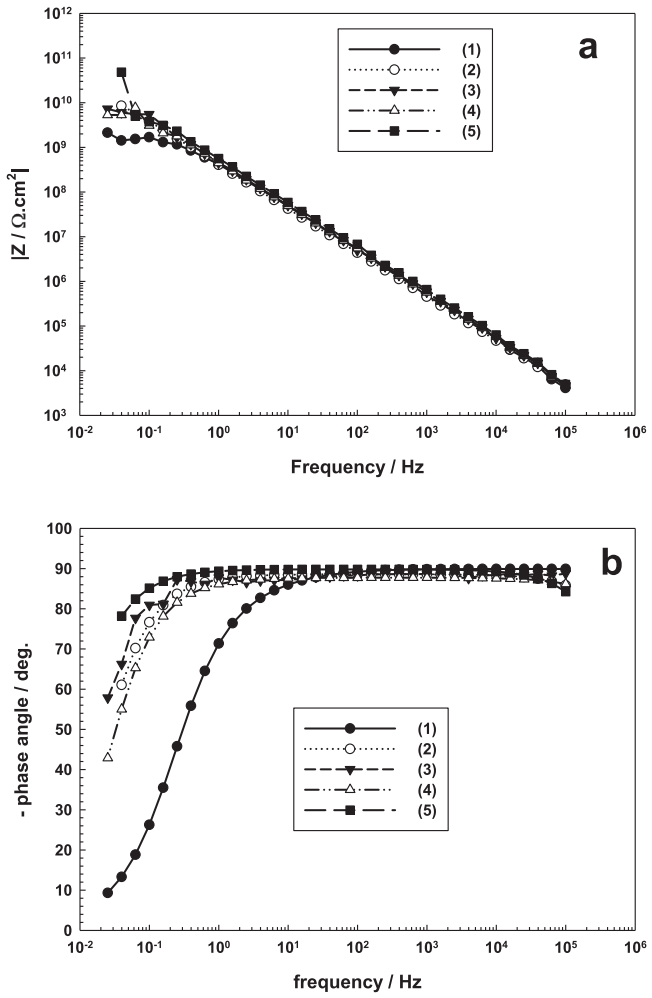

Fig. 5. EIS plots Bode modulus (**a**) and Bode phase (**b**) plots after immediate immersion of different coating formulations. PU clear coating **(1)**; PU+ 1 % wt. (Bi, Ca, Zn)VO_4 calcined at 500 °C (**2**); PU+ 1 % wt. (Bi, Ca, Zn)VO_4 calcined at 550 °C (**3**); PU+ 1 % wt. (Bi, Ca, Zn)VO_4 calcined at 600 °C (**4**); PU+ 1 % wt. (Bi, Ca, Zn)VO_4 calcined at 650 °C (**5**).

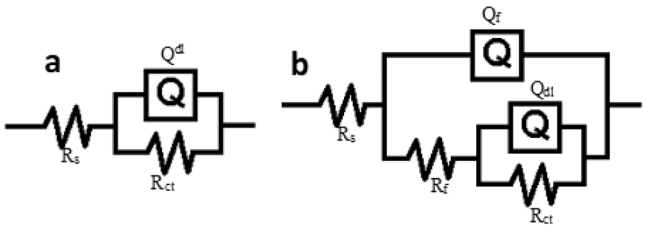

Fig. 6. Equivalent circuits of coated metal. (**a**): Equivalent circuits of the coated metal system at the very first time of immersion. (**b**): Equivalent circuits of the coated metal for long immersion time.

barrier corrosion for steel substrate.

For PU clear coating without pigment, the impedance modulus at 0.01 Hz is about 2.13×10^{10} Ω.cm^2 immediately after immersion (Fig. 7**a**). It progressively decreases with increasing immersion time and reaches 4.08×10^7 Ω.cm^2 after 720 h in the aggressive medium. The phase angle displays a marked decrease at medium and low-frequency range, and two-time constants were observed in the Bode plot. The relatively high impedance modulus at low frequency at the first time of immersion in the electrolyte indicates that the barrier properties of the polyurethane coating without pigment are good. However, the progressive decrease of the impedance modulus at low frequency and the appearance of a second time constant after 24 h immersion in the electrolyte reveal a charge transfer reaction at the interface between the coating and steel substrate [31]. These results indicate that polyurethane coatings containing 1 % wt. of all calcined pigment particles provide high impedance modulus during immersion in the 0.5 NaCl solution. This sustains good barrier performance of PU base coatings containing (Bi, Ca, Zn)VO_4 powder. The performance of the corrosion resistance of the coating probably takes advantage of the presence of Zn^{2+} ions containing pigment in the polymeric coating matrix. The process can be explained considering the electrochemical theory: the anodic oxidation of the metal and the cathodic reduction of dissolved oxygen. The metal atoms release electrons at the anodic area and dissolve as ions in the solution. For steel substrate, the oxidation reactions are as follows:

$$Fe \longrightarrow Fe^{2+} + 2e^- \; and \; Fe^{2+} \longrightarrow Fe^{3+} + e^-$$

At the cathodic area occurs the reduction of dissolved oxygen:

$$O_2 + 2H_2O + 4e^- \longrightarrow 4OH^-$$

The pigment particles can release the Zn^{2+} cations which reach with OH^- ions at the cathodic sites, at coating/metal, leading to the formation of compact ZnO protective layer which inhibits blocked the access aggressive species as the following equation:

$$Zn^{2+} + 2OH^- \longrightarrow Zn(OH)_2 \longrightarrow ZnO + H_2O$$

This result agrees with previous works on the protective properties enhancement of polyurethane coatings [32–35] and epoxy-polyamide [36–37]. They found that the adhesion strength, hardness, and cross-link for composite coating after exposure to corrosive electrolyte was remarkably higher than pure epoxy coating. Moreover, Zuo and co-workers showed that epoxy primer coatings loaded with Zn-containing particles exhibit an improvement in the physical crosslink density of the epoxy coating, enhancement of anti-corrosion performance, and adhesion strength [38]. To establish the light stability of the (Bi,Ca,Zn)VO_4 pigments used in the paint, an UV-B exposure has been conducted. Gloss evolution has been recorded at different exposure times (Fig. 8). A slight change in gloss was observed for all pigmented coating, indicating a very low sensitivity of the coatings to UV-B radiation.

Considering these results, it appears that the unpigmented coating exhibits a marked decrease in gloss during the first ten days of exposure; after this, the gloss remains stable during the twenty following days. For pigmented coatings, the PU+ 1 % wt. pigment calcined at 500 °C exhibited the lowest change in gloss during the thirty days of UV-B exposure. The two other coating systems, although showing a slight evolution in gloss during the first ten days, showed a drastic decrease in gloss between the tenth and twentieth days of UV-B exposure. FTIR spectra were also recorded at different times to evaluate the chemical changes due to UV-B exposure. Fig. 9 shows the FTIR spectra of pigmented coating samples with 1 wt% pigment load (left) and clear coating of the base paint (right). The spectra were recorded at three UV-B exposure times (0, 240, and 720 h). For the pigmented coating, the OH vibration band around 3300 cm^{-1} showed a significant broadening with the UV-B exposure time. This can be attributed to a generation of carboxylic acids, indicating an aging process [39–41] that took place much faster than for the unpigmented paint. Furthermore, a progressive reduction of stretching aliphatic C–H peaks at 2987–2743 cm^{-1} was also observed in pigmented and clear coatings. These peaks almost disappeared after 720 h of UV-B testing time. This suggests that exposure to UV-B tended to decrease the molecular weight of the binder material due to photooxidative reactions [41].

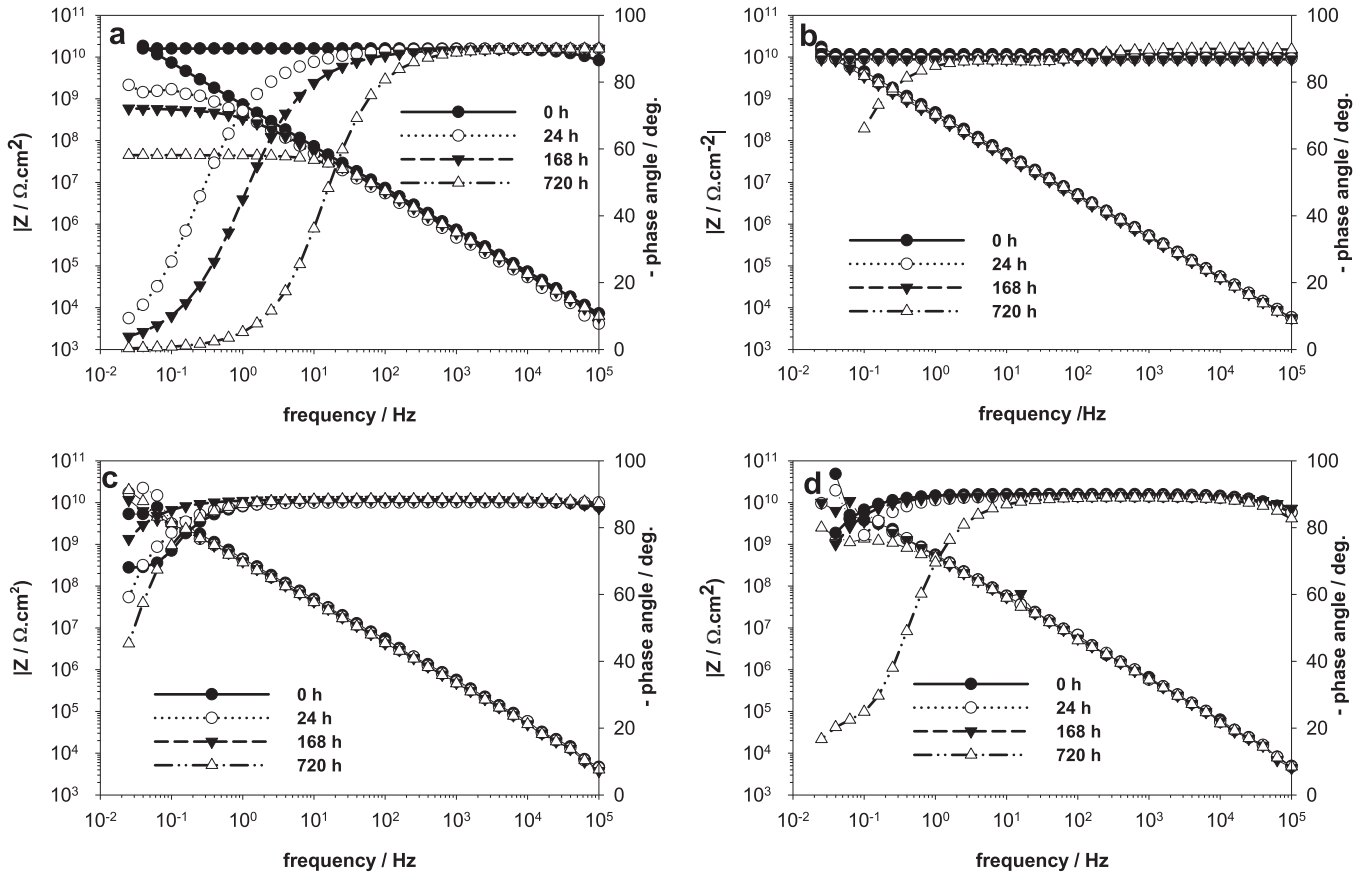

Fig. 7. impedance modulus and phase angle plots for steel panel coated with PU base coating loaded with 1 % wt. (Bi, Ca, Zn)VO_4 pigment calcined for different temperature in 0.5 M. NaCl solution as a function of immersion time. (**a**): PU clear coating; (**b**): 1 % wt. (Bi, Ca, Zn)VO_4 calcined at 500 °C; (**c**): 1 % wt. (Bi, Ca, Zn)VO_4 calcined at 600 °C; (**d**): 1 % wt. (Bi, Ca, Zn)VO_4 calcined at 650 °C;.

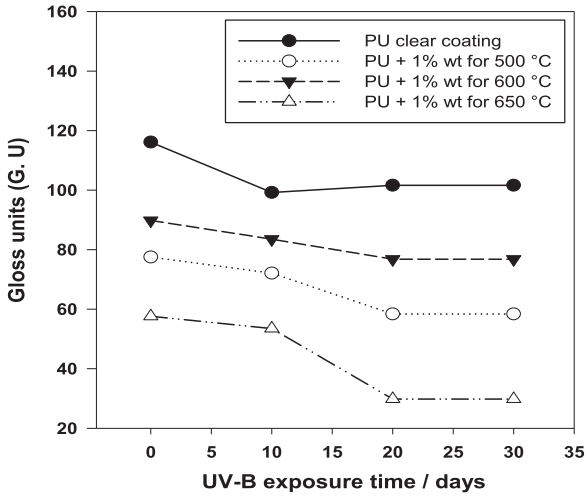

Fig. 8. Evolution of 60° gloss units as a function of UV-B exposure time.

4. Conclusion

This study evaluated the protective barrier property, color stability, and UV-B resistance of a coating system formulated with polyurethane base paint and eco-friendly (Bi, Zn, Ca)VO_4 inorganic yellow pigment. The pigment has been synthesized according to the previous work of T Masui. Its yellowness depends on the calcination temperature of the precipitate obtained after the sol-gel process. The most vivid tint was obtained for a calcination temperature of about 500 °C, with color parameters of L* = 84.6, a* = 5.20, and b* = 88.60. The b* value is significantly higher than a commercial $BiVO_4$ pigment (b* = +76.9). As this pigment is expected to be a promising alternative to toxic yellow pigments with environmentally friendly properties, we formulated a coating system by mixing 1 % wt. of the inorganic pigments with a polymeric-based binding material. The EIS response of pigmented coating systems indicated a capacitive behavior for the 720 h immersion test. Pigmented coatings exhibited higher and more stable barrier properties than the unpigmented coating system. This indicates that the

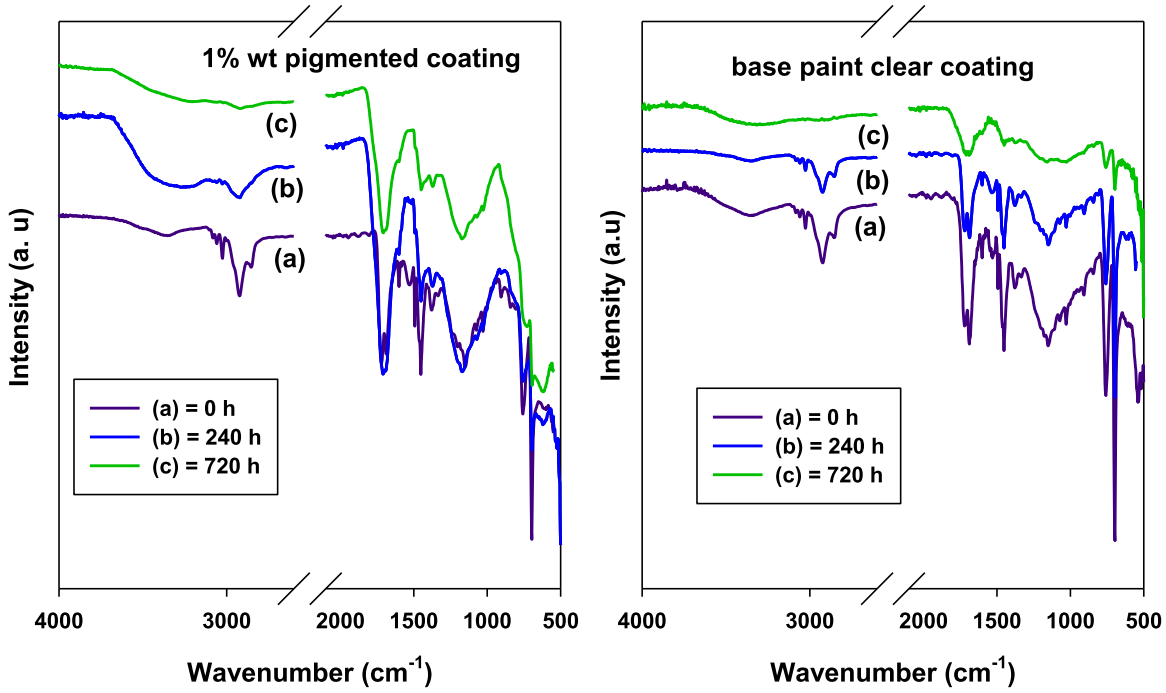

Fig. 9. FTIR spectra for each PU containing 1 wt% pigment and clear coat.

mineral presents good compatibility with polyurethane polymer, enhances the interactions at the interface between polymeric material and substrate, provides a more resistive path for the diffusion of aggressive species (oxygen, chloride ions…) within polymer coating, and improves the corrosion performance of the coatings. Continuous long-time immersion test performed with EIS indicated good stability of pigmented coating in the aggressive 0.5 M solution. The color and gloss parameters of the pigmented coating sample remained relatively stable after 720 h of UV-B exposure. Nevertheless, the FTIR analyses showed that the pigmented coating was sensitive to some photooxidation processes.

CRediT authorship contribution statement

Stefano Rossi: Writing – review & editing, Visualization, Validation, Supervision, Software, Resources, Formal analysis. **Tambi Ramdé:** Writing – original draft, Validation, Software, Investigation, Funding acquisition, Formal analysis, Conceptualization. **Mamadou Ouédraogo:** Writing – original draft, Investigation, Data curation. **Boubié Guel:** Resources, Funding acquisition.

Declaration of Competing Interest

The authors declare the following financial interests/personal relationships which may be considered as potential competing interests: OUEDRAOGO Mamadou reports financial support was provided by International Science Program. If there are other authors, they declare that they have no known competing financial interests or personal relationships that could have appeared to influence the work reported in this paper.

Acknowledgment

The authors thank Dr Massimo Calovi and Mr. Luca Benedetti for their help in the experiment. The authors thank the International Science Program (Sweden) for financial support through the project IPICS/ISP/BUF:02.

References

[1] T. Masui, T. Honda, Wendusu, N. Imanaka, Novel and environmentally friendly (Bi, Ca, Zn)VO_4 yellow pigments, Dyes Pigments 99 (2013) 636–641, https://doi.org/10.1016/j.dyepig.2013.06.030.
[2] A. Gürses, M. Açıkyıldız, K. Güneş, M.S. Gürses, Classification of dye and pigments. Dyes and Pigments; Springer Briefs in Molecular Science, Springer, Cham, 2016, https://doi.org/10.1007/978-3-319-33892-7_3.
[3] A. Kalendova, D. Vesely, J. Stejskal, Organic coatings containing polyaniline and inorganic pigments as corrosion inhibitors, Prog. Org. Coat. 62 (2008) 105–116, https://doi.org/10.1016/j.porgcoat.2007.10.001.
[4] P.A. Lewis; Inorganic colored pigments. paint and coating testing manual: 15th. Edition of the Gardner-Sward Handbook. Ed. Koleske. JV. 100 Barr Harbor Drive. PO Box C700. West Conshohocken. PA 19428-2959: ASTM International. 2012; DOI: https://doi.org/10.1520/MNL12202M.
[5] G. Pfaff, The world of inorganic pigments, Chem. Texts 8 (2022) 15, https://doi.org/10.1007/s40828-022-00166-1.
[6] L. Cao, X. Fei, H. Zhao, Environmental substitution for $PbCrO_4$ pigment with inorganic-organic hybrid pigment, Dyes Pigments 142 (2017) 100–107, https://doi.org/10.1016/j.dyepig.2017.03.024.
[7] S. Sameera, P.P. Rao, S. Divya, K.V. Athira, T.R. Raj, A. Thara, High IR reflecting $BiVO_4$-$CaMoO_4$ based yellow pigments for cool roof applications, Energy Build. 154 (2017) 491–498, https://doi.org/10.1016/j.enbuild.2017.08.089.
[8] M. Jansen, H.P. Letschert, Inorganic yellow-red pigments without toxic metals, Nature 404 (6781) (2000) 980–982, https://doi.org/10.1038/35010082.
[9] B. Kumar, R. Sharma, H. Bhoi, K. Punia, S. Kumar, S.K. Barbar, Synthesis. structural. morphological and optical properties of environment friendly yellow inorganic pigment $Bi_4Zr_3O_{12}$, Opt. Mater. 143 (2000) 114040, https://doi.org/10.1016/j.optmat.2023.114040.
[10] I. Rus, R. Ianoș, R. Lazau, C. Pacurariu, New blue pigments based on Co^{2+} and La^{3+} doped hibonite for NIR-reflective coatings, Mater. Today Chem. 28 (2023) 101391, https://doi.org/10.1016/j.mtchem.2023.101391.
[11] X. Zhou, M.-H. Zhao, J. Yang, Y. Han, L. Cao, Y.-Y. Han, J. Wang, Y. Wang, M.-R. Li, Chemical pressure enlarged camouflage color zone in Mn(IV)-activated yellow-green pigments, Mater. Today Chem. 25 (2022) 100902, https://doi.org/10.1016/j.mtchem.2022.100902.
[12] S. Li, B. Mu, Z. Meng, Y. Zhu, H. Zhang, A. Wang, Facile color regulation of organic/inorganic hybrid pigments combining with palygorskite and CoNi layered double hydroxides, Dyes Pigments 213 (2023) 111162, https://doi.org/10.1016/j.dyepig.2023.111162.
[13] K. Ohnishi, R. Oka, Y. Nomura, T. Masui, A novel inorganic violet pigment based on zinc niobate, Mater. Adv. 4 (2023) 1583–1589, https://doi.org/10.1039/D3MA00040K.
[14] B. Lehr, G. Zurowski, J. Chhoeun, K. Kumar, G. Nolis, J. Shanahan, K. Kilpatrick, K. Rojas, J. Cabana, D. Kissel, M. Avdeev, E. Sullivan, Mater. Res. Bull. 174 (2024) 112746, https://doi.org/10.1016/j.materresbull.2024.112746.
[15] P.K. Thejus, K.V. Krishnapriya, K.G. Nishanth, A cost-effective intense blue colour inorganic pigment for multifunctional cool roof and anticorrosive coatings, Sol.

Energy Mater. Sol. Cells 219 (2021) 110778, https://doi.org/10.1016/j.solmat.2020.110778.
[16] R. Nayak, A. Suryanarayana, S.B. Rao, Synthesis. Characterization and testing of bismuth vanadate – an eco-friendly yellow pigment, J. Sci. Ind. Res. 59 (2000) 833–837. ⟨http://nopr.niscpr.res.in/handle/123456789/26621⟩.
[17] H. EndrissHigh Performance Pigments; Ed. Edwin B. Faulkner. Russell J. Schwartz, 2009. 7–12; http://doi.org/10.1002/9783527626915.ch2.
[18] L.S. Kumari, P.P. Rao, A.N.P. Radhakrishnan, V. James, S. Sameera, P. Koshy, Brilliant yellow color and enhanced NIR reflectance of monoclinic $BiVO_4$ through distortion in VO_4^{3-} tetrahedra, Sol. Energy Mater. Sol. Cells 112 (2013) 134–143, https://doi.org/10.1016/j.solmat.2013.01.022.
[19] S. Furukawa, T. Masui, N. Imanaka, Synthesis of new environment-friendly yellow pigments, J. Alloy. Compd. 418 (2006) 255–258, https://doi.org/10.1016/j.jallcom.2005.08.108.
[20] V.J. Patil, Y.E. Bhoge, U.D. Patil, T.D. Deshpande, R.D. Kulkarni, Room temperature solution spray synthesis of Bismuth Vanadate nanopigment and its utilization in formulation of industrial OEM coatings, Vacuum 127 (2016) 17–21, https://doi.org/10.1016/j.vacuum.2016.02.005.
[21] Q. Peng, Z. Wang, B. Xie, D. Chen, J. Jian, H. Wang, Simultaneous intramolecular and intermolecular coupling of polar bond vibrations induced spectral splitting phenomenon, J. Mol. Liq. 401 (2024) 124719, https://doi.org/10.1016/j.molliq.2024.124719.
[22] N.H. Al-Jallo, F.N. Al-Azawi, Study of Fermi resonance in ethylene carbonate by the method of isotopic substitution, Spectrochim. Acta 34A (1977) 819–823, https://doi.org/10.1016/0584-8539(78)80036-1.
[23] A.A. Kananenka, J.L. Skinner, Fermi resonance in OH-stretch vibrational spectroscopy of liquid water and the water hexamer, J. Chem. Phys. 148 (2018) 244107, https://doi.org/10.1063/1.5037113.
[24] T.T. Bui, L.A. Colon, L. Velarde, Intermolecular Interactions at the silica-liquid Interface modulate the Fermi resonance coupling in surface methanol, J. Phys. Chem. Lett. 12 (2021) 5695, https://doi.org/10.1021/acs.jpclett.1c01015.
[25] S. Zhang, H. Jia, M. Song, H. Shen, D. Li, H. Li, Raman spectroscopy study of acetonitrile at low temperature, Spectrochim. Acta Part a-Mol. Biomol. Spectrosc. 246 (2021) 119065, https://doi.org/10.1016/j.saa.2020.119065.
[26] X. Zhang, T. Chen, Y. Xu, W. Jiang, J. Liu, Z. Xie, Synthesis and characterization of environmentally friendly $BiVO_4$ yellow pigment by non-hydrolytic sol-gel route, J. Sol. -Gel Sci. Technol. 91 (2019) 127–137, https://doi.org/10.1007/s10971-019-05026-y.
[27] S.-W. Ge, P. Hu, J. Deng, et al., The effect of secondary phase on corrosion behaviors of the titanium–zirconium–molybdenum alloy, Tungsten 6 (2024) 342–354, https://doi.org/10.1007/s42864-023-00228-y.
[28] I.C.P. Margarit-Mattos, EIS and organic coatings performance: revisiting some key points, Electrochim. Acta 354 (2020) 136725, https://doi.org/10.1016/j.electacta.2020.136725.
[29] J.B. Jorcin, M.E. Orazem, N. Pébère, B. Tribollet, CPE analysis by local electrochemical impedance spectroscopy, Electrochim. Acta 51 (2006) 1473, https://doi.org/10.1016/j.electacta.2005.02.128.
[30] P.H. Bottelberghs, G.H.J. Broers, Interfacial impedance behaviour of polished and paint platinum electrodes at Na2WO4-Na2MoO4 solid electrolytes, J. Electroanal. Chem. 67 (1976) 155, https://doi.org/10.1016/S0022-0728(76)80332-4.
[31] B. Ramezanzadeh, M. Attar, Studying the effects of micro and nano sized ZnO particles on the corrosion resistance and deterioration behavior of an epoxy-polyamide coating on hot-dip galvanized steel, Prog. Org. Coat. 71 (2011) 314–328, https://doi.org/10.1016/j.porgcoat.2011.03.026.
[32] G. Christopher, M.A. Kulandainathan, G. Harichandran, Highly dispersive waterborne polyurethane/ZnO; nanocomposites for corrosion protection, J. Coat. Technol. Res. 12 (4) (2015) 657–667, https://doi.org/10.1007/s11998-015-9674-3.
[33] M. Rashvand, Z. Ranjbar, Effect of nano-ZnO particles on the corrosion resistance of polyurethane-based waterborne coatings immersed in sodium chloride solution via EIS technique, Prog. Org. Coat. (2013) 1413–1417, https://doi.org/10.1016/j.porgcoat.2013.04.013.
[34] N. Arianpouya, M. Shishesaz, M. Arianpouya, M. Nematollahi, Evaluation of synergistic effect of nanozinc/nanoclay additives on the corrosion performance of zinc-rich polyurethane nanocomposite coatings using electrochemical properties and salt spray testing, Surf. Coat. Technol. 216 (2013) 199–206, https://doi.org/10.1016/j.surfcoat.2012.11.036.
[35] K. Lau, S. Permeh, Assessment of durability and zinc activity of zinc-rich primer coatings by electrochemical noise technique, Prog. Org. Coat. 167 (2022) 106840, https://doi.org/10.1016/j.porgcoat.2022.106840.
[36] M. Rashvand. Z. Ranjbar. S. Rastegar; Preserving anti-corrosion properties of epoxy based coatings simultaneously exposed to humidity and UV-radiation using nano zinc oxide; J. Electrochem. Soc. 159 C129; https://doi.org/10.1149/2.093203jes.
[37] M. Anghelone, D. Jembrih-Simbürger, M. Schreiner, Influence of phthalocyanine pigments on the photo-degradation of alkyd artists' paints under different conditions of artificial solar radiation, Polym. Degrad. Stab. 134 (2016) 157–168, https://doi.org/10.1016/j.polymdegradstab.2016.10.007.
[38] A. Zuo, Y. Huang, X. Xu, Y. Su, S. Liu, Y. Tang, Degradation behavior of zinc-rich epoxy coatings in simulated marine tidal zone, Mater. Today Commun. 38 (2024) 108175, https://doi.org/10.1016/j.mtcomm.2024.108175.
[39] R. Ploeger, D. Scalarone, O. Chiantore, The characterization of commercial artists' alkyd paints, J. Cult. Herit. 9 (4) (2008) 412–419, https://doi.org/10.1016/j.culher.2008.01.007.
[40] V. Pintus, S. Wei, M. Schreiner, Accelerated UV ageing studies of acrylic, alkyd, and polyvinyl acetate paints: influence of inorganic pigments, Microchem. J. 124 (2016) 949–961, https://doi.org/10.1016/j.microc.2015.07.009.
[41] S. Rossi, H. Lindmark, M. Fedel, Colored paints containing NIR-reflective pigments exposed to accelerated ultraviolet radiation aging with possible application as roof coatings, Coatings 10 (2020) 1135, https://doi.org/10.3390/coatings10111135.